



HAL
open science

Injectable Self-Healing Hydrogels Based on Boronate Ester Formation between Hyaluronic Acid Partners Modified with Benzoxaborin Derivatives and Saccharides

Tamiris Figueiredo, Jing Jing, Isabelle Jeacomine, Johan Olsson, Thibaud Gerfaud, Jean-Guy Boiteau, Claire Rome, Craig Harris, Rachel Auzély-Velty

► **To cite this version:**

Tamiris Figueiredo, Jing Jing, Isabelle Jeacomine, Johan Olsson, Thibaud Gerfaud, et al.. Injectable Self-Healing Hydrogels Based on Boronate Ester Formation between Hyaluronic Acid Partners Modified with Benzoxaborin Derivatives and Saccharides. *Biomacromolecules*, 2020, 21 (1), pp.230-239. 10.1021/acs.biomac.9b01128 . hal-03794022

HAL Id: hal-03794022

<https://hal.science/hal-03794022v1>

Submitted on 7 Oct 2022

HAL is a multi-disciplinary open access archive for the deposit and dissemination of scientific research documents, whether they are published or not. The documents may come from teaching and research institutions in France or abroad, or from public or private research centers.

L'archive ouverte pluridisciplinaire **HAL**, est destinée au dépôt et à la diffusion de documents scientifiques de niveau recherche, publiés ou non, émanant des établissements d'enseignement et de recherche français ou étrangers, des laboratoires publics ou privés.

1 Injectable self-healing hydrogels based on boronate
2 ester formation between hyaluronic acid partners
3 modified with benzoxaborin derivatives and
4 saccharides

5 *Tamiris Figueiredo,[‡] Jing Jing,[†] Isabelle Jeacomine,[‡] Johan Olsson,[§] Thibaud Gerfaud,[†] Jean-*
6 *Guy Boiteau,[†] Claire Rome,[¥] Craig Harris,[†] Rachel Auzély-Velty^{‡*}*

7 [‡]Univ. Grenoble Alpes, Centre de Recherches sur les Macromolécules Végétales (CERMAV)-
8 CNRS, 601, rue de la Chimie, BP 53, 38041 Grenoble Cedex 9 (France)

9 [†]Galderma/Nestlé Skin Health R&D, 2400 Route de Colles, 06410 Biot (France)

10 [§]Galderma/Nestlé Skin Health R&D, Seminariegatan 21, SE-752 28 Uppsala (Sweden)

11 [¥]Univ. Grenoble-Alpes, Institut des Neurosciences (GIN), Bâtiment Edmond J. Safra, Chemin
12 Fortuné Ferrini, 38706 La Tronche Cedex (France)

13

14 **Abstract**

15 We demonstrate here, for the first time, formation of injectable dynamic covalent hydrogels at
16 physiological pH using benzoxaborin-saccharide complexation as a reversible crosslinking

1 method. The gels were prepared by simply mixing hyaluronic acid modified with an original
2 boronic acid derivative, 3,4-dihydro-2H-benzo[e][1,2]oxaborinin-2-ol (1,2-ABORIN), and HA
3 functionalized with 1-amino-1-deoxy-D-fructose. Dynamic rheological experiments confirmed
4 the gel-like behavior (storage modulus (G') > loss modulus (G'') in the frequency window
5 explored) for the designed HA-1,2-ABORIN/HA-fructose network. Furthermore, this hydrogel
6 exhibited excellent self-healing and injectability behaviors in aqueous conditions and was found
7 to be responsive to pH. Additionally, fibroblast cells encapsulated in the HA network showed
8 high viability (> 80 % after 7 days of cell culture), as monitored by Live/Dead staining. Taken
9 together, this new class of boronate ester crosslinked hydrogel provides promising future for
10 diverse biomedical applications.

11 KEYWORDS: Self-healing, injectable hydrogel, benzoxaborin-saccharide dynamic covalent
12 cross-linking, cell delivery.

13 **Introduction**

14 Recent advances in biomaterials research have encouraged the design of new injectable
15 hydrogels with autonomous self-healing properties, i.e. having the ability to response to damage
16 and regenerate function, without requiring the application of external physical or chemical
17 stimuli.¹⁻³ Such polymer networks can be pre-formed into syringes, extruded under application of
18 shear (needle injection), and rapidly recover the gel state when the applied stress is removed.⁴
19 These materials have become particularly attractive for clinical uses as they can be surgically
20 implanted in patients by minimally invasive methods. Such hydrogels can be crosslinked via
21 non-covalent interactions (e.g. hydrophobic, hydrogen bonding, ionic, host-guest interactions) or
22 dynamic covalent bonds.⁵ Among the latter, the boronic ester bond has presented great potential

1 to prepare self-healing hydrogels as biomimetic scaffolds for cell encapsulation.⁶⁻⁹ As the
2 formation of crosslinks in these gels at physiological pH strongly depends on the affinity of the
3 boronic acid towards the diol (K_a) and on their pK_a ,¹⁰ their stiffness as well as their dynamics
4 may be tuned by varying the nature of the boronic acid moiety⁹ and/or the diol-containing
5 molecule.^{8,11}

6 Inspired by studies on the structure-property relationships of small arylboronic acid
7 molecules,¹²⁻¹⁶ several boronate-crosslinked hydrogels have been thus prepared at physiological
8 pH using phenylboronic acid (PBA)¹⁷⁻¹⁹ and its derivatives, such as PBA substituted with
9 fluorine as an electron-withdrawing group that can reduce pK_a ,^{6,9} and *ortho*-substituted PBA
10 derivatives,²⁰ in particular *o*-hydroxymethylphenylboronic acid (benzoboroxole, BOR, Figure
11 1).^{11,21,22} Compared to PBA, BOR has a strained five-membered oxaborole ring, which is a
12 contributing factor explaining its higher acidity (pK_a of 7.3¹⁴) than PBA (pK_a of 8.8²³) and its
13 exceptional carbohydrate-binding behavior at neutral pH.^{16,24} The capability of this class of
14 arylboronic acid to bind non-reducing saccharides locked in their pyranose form
15 (glycopyranosides) was first reported by the Hall group.^{15,25} This unique property was
16 successfully used to produce highly elastic hydrogel networks, exhibiting slow dynamics, and
17 crosslinked via complexation of BOR with mannopyranoside moieties covalently linked to
18 synthetic polymers.¹¹

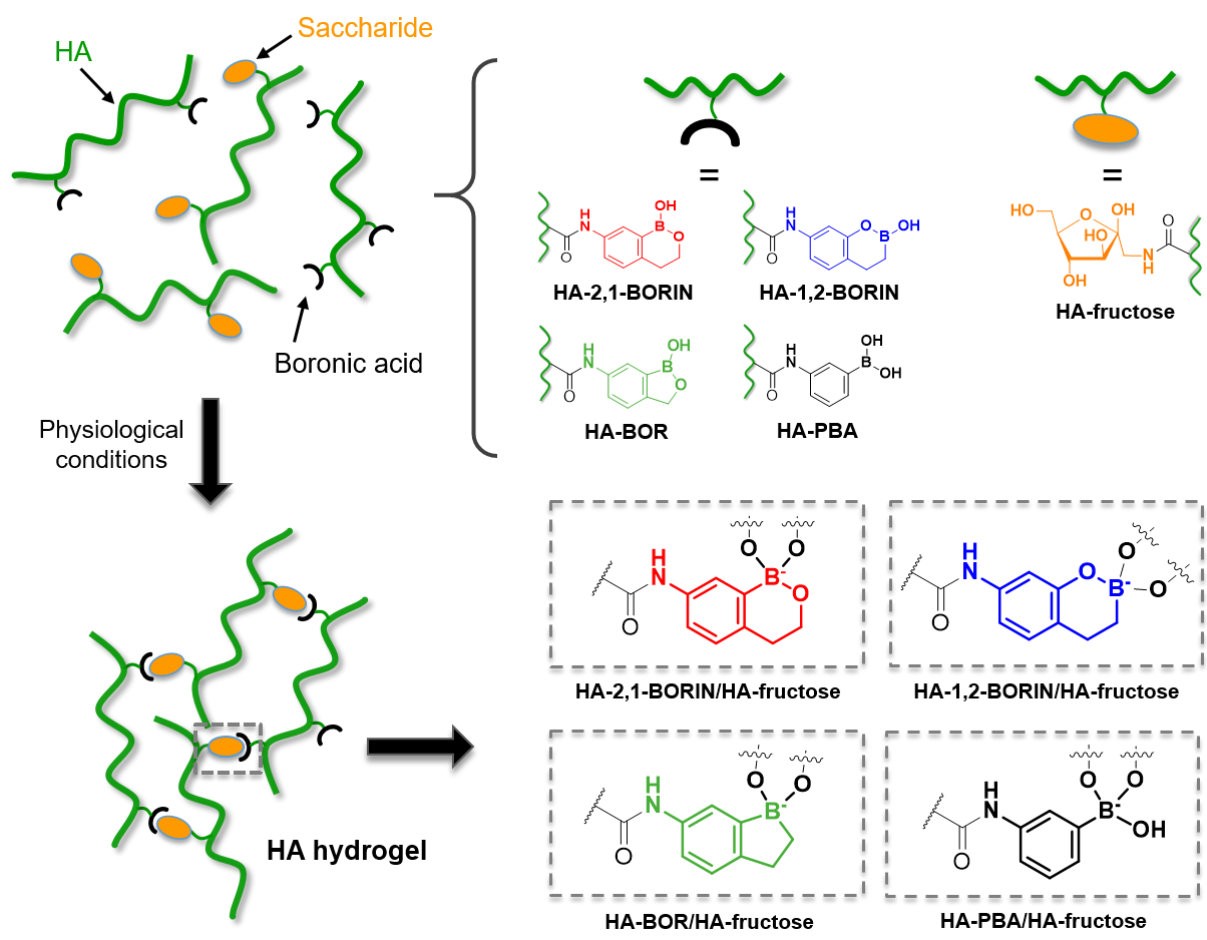
19 In addition to benzoboroxole, its six-membered ring homologue, *o*-
20 hydroxyethylphenylboronic acid (benzoxaborin, 2,1-BORIN, Figure 1), has recently been
21 investigated as a synthetic building block for constructing bioactive molecules,^{14,26,27} and as a
22 recognition element for carbohydrate sensing.²⁵ However, in spite of the structural similarities
23 between BOR and 2,1-BORIN, the latter is not able to complex saccharides in the pyranose form

1 at neutral pH.²⁵ Indeed, studies published by Tomsho *et al.* explain the different binding
2 capacities of these derivatives based on their geometrical structures.¹⁴ Regarding 2,1-BORIN, its
3 less strained six-membered ring, compared to the strained five-membered ring of BOR, does not
4 induce a distorted geometry around the boron atom, which results in a less reactive boronic
5 center and a higher pK_a (8.4).¹⁴ On the other hand, the slightly higher acidity of 2,1-BORIN in
6 comparison with PBA appears to be related to a reduced flexibility of the intramolecular B-O
7 bond of the former, which increases boron electronic deficiency. Nevertheless, despite increasing
8 attention has been paid to assess the potential of benzoxaborin compounds as sugar-binding
9 agents, no published studies have exploited benzoxaborin-saccharide complexation as a
10 crosslinking strategy to form reversible boronate ester-crosslinked hydrogels.

11 The present study is a first demonstration of the applicability of dynamic benzoxaborin-
12 saccharide complexation as a reversible crosslinking method to form hyaluronic acid networks at
13 physiological pH. As illustrated in Figure 1, besides 2,1-BORIN, a new original derivative called
14 1,2-benzoxaborin (1,2-BORIN), containing a six-membered heterocycle like 2,1-BORIN but
15 with the endocyclic oxygen linked to the phenyl ring, was also investigated as a binding site for
16 D-fructose grafted on HA. Herein, D-fructose was selected to form reversible crosslinks with the
17 benzoxaborin derivatives due to its higher affinity for arylboronic acids in comparison to other
18 classical monosaccharides.^{28,29} Although the 1,2-BORIN molecule has never been tested and
19 reported in the literature as a carbohydrate-binding agent, we hypothesized that its particular
20 structure would provide a more acidic character to boronic acid (i.e. lower pK_a) compared to
21 standard 2,1-BORIN, favoring its complexation with D-fructose at physiological pH.

22 In this work, the formation of HA hydrogel networks through reversible benzoxaborin-
23 fructose complexation was investigated and the dynamic rheological properties of the designed

1 networks were compared to those obtained by mixing the HA-fructose conjugate with HA
 2 bearing BOR or PBA moieties. Their injectability and self-healing properties were further
 3 evaluated in detail by rheology and injection force measurements. Lastly, their suitability and
 4 biocompatibility for cell and tissue engineering was demonstrated by 3D encapsulation of
 5 fibroblast cells.



6
 7 **Figure 1.** HA hydrogels crosslinked by boronic acid-fructose complexation at physiological pH.
 8 Hydrogel formation is triggered by combining fructose-grafted HA and HA modified with
 9 benzoxaborin derivatives (2,1-BORIN and 1,2-BORIN), benzoboroxole (BOR) or phenylboronic
 10 acid (PBA).

1
2
3
4
5
6
7
8
9
10
11
12
13
14
15
16
17
18
19
20
21
22

Experimental section

Materials. Sodium hyaluronate (HA) possessing a weight-average molar mass (M_w) of 360 kg/mol was donated by Galderma-Nestlé Skin Health. The molar mass distribution and the weight-average molar mass of these samples were determined by size exclusion chromatography using a Waters GPC Alliance chromatograph (USA) equipped with a differential refractometer and a light scattering detector (MALLS) from Wyatt (USA); the solution was injected at a concentration of 1×10^{-3} g/mL in 0.1 M NaNO₃, at a flow rate of 0.5 mL/min and at a column temperature of 30 °C. The dispersity (D) of the samples are $M_w/M_n \approx 1.5-2$. The overlap concentration C^* for the HA sample in buffer at 25 °C is around 1 g/L. This value was derived from the intrinsic viscosity assuming that $C^*[\eta]$ is about unity.³⁰ A HA sample with a lower M_w (5 kg/mol), purchased from the same supplier, was used to synthesize HA derivatives for NMR studies (determination of binding constants). This low M_w HA sample was used to circumvent limitations due to the high viscosity of concentrated solutions of high M_w HA. 5-Amino-2-hydroxymethylphenylboronic acid (6-aminobenzoboroxole, ABOR) was purchased from Combi-Blocks. 1-Amino-1-deoxy-D-fructose hydrochloride (fructosamine) was supplied by Carbosynth. 3-Aminophenylboronic acid hemisulfate salt (APBA), 4-(4,6-dimethoxy-1,3,5-triazin-2-yl)-4-methylmorpholinium chloride (DMTMM), picrylsulfonic acid solution (TNBS), 4-(2-hydroxyethyl)piperazine-1-ethanesulfonic acid (HEPES), phosphate buffered saline (PBS) and other chemicals were purchased from Sigma-Aldrich-Fluka and were used without further purification.

Methods.

1 **NMR spectroscopy.** ^1H , ^{13}C and ^{11}B NMR spectra were recorded at 25 °C or 80 °C using a
2 Bruker AVANCE III HD spectrometer operating at 400.13 MHz (^1H), 100.61 MHz (^{13}C) and
3 128.38 MHz (^{11}B). ^1H NMR spectra were recorded by applying a 90° tip angle for the excitation
4 pulse, and a 10 s recycle delay for accurate integration of the proton signals. ^{13}C NMR spectra
5 were recorded by applying a 90° tip angle for the excitation pulse and a 2 s recycle delay.
6 Deuterium oxide (D_2O) was obtained from Euriso-top (Saint-Aubin, France). Chemical shifts (δ
7 in ppm) are given relative to external tetramethylsilane (TMS = 0 ppm) and calibration was
8 performed using the signal of the residual protons of the solvent as a secondary reference. All
9 NMR spectra were analyzed with Topspin 3.1 software from Bruker AXS.

10 **Determination of the $\text{p}K_a$ of 1,2-ABORIN and 2,1-ABORIN by ^{11}B NMR spectroscopy.** ^{11}B
11 NMR chemical shifts of the aminobenzoxaborin compounds were determined with increasing pH
12 (10 % D_2O in H_2O , 16 mM in 0.01 M phosphate buffer). Chemical shifts (δ in ppm) for each ^{11}B
13 spectrum were given relative to external $\text{Et}_2\text{O}\text{-BF}_3$ in deuterated chloroform as zero. The values
14 of $\text{p}K_a$ were determined from the curve fitting of the variation of δ (in ppm) with the pH using
15 the Boltzmann equation (Figures 4a and 4b).

16 **Synthesis of HA derivatives.** HA-1,2-BORIN, HA-2,1-BORIN, HA-PBA, HA-BOR and HA-
17 fructose were synthesized by an amide coupling reaction from 1,2-ABORIN, 2,1-ABORIN,
18 APBA, ABOR and fructosamine (containing free primary amine groups), respectively. To this
19 end, 1,2-ABORIN (0.026 g, 0.12 mmol) or 2,1-ABORIN (0.0205 g, 0.12 mmol) or APBA (0.022
20 g, 0.12 mmol) or ABOR (0.025 g, 0.135 mmol) or fructosamine (0.024 g, 0.112 mmol) was
21 added to a water/DMF (3/2, v/v) mixture containing DMTMM (0.207 g, 0.75 mmol) and HA
22 (0.3 g, 0.75 mmol) and the pH was adjusted to 6.5 using 0.5 M aqueous NaOH. After stirring for
23 24 h at room temperature, the different HA derivatives were purified by ultrafiltration using

1 deionized water and the products were recovered by freeze-drying (Table 1). The DS of the HA
2 derivatives were found to be 0.1-0.15 from ^1H NMR analyses (Figure S1-S4) or from the
3 reaction kinetics using the TNBS method (Figure S6).

4 **Table 1.** Reaction conditions for the synthesis of HA360 conjugates.

HA derivative	R-NH ₂ /HA molar ratio	DS	Coupling (%)	Yield (%)
HA-1,2-BORIN	0.16	0.15 ^{a)}	94	81
HA-2,1-BORIN	0.16	0.15 ^{a)}	94	90
HA-BOR	0.16	0.1 ^{a)}	75	91
HA-PBA	0.16	0.15 ^{a)}	94	98
HA-fructose	0.15	0.15 ^{b)}	100	96

5 ^{a)}DS by ^1H NMR (10 % of accuracy).

6 ^{b)}DS estimated from the reaction kinetics using TNBS.

7 **Preparation of HA-1,2-BORIN (HA-2,1-BORIN or HA-BOR or HA-PBA) and HA-fructose**
8 **mixtures.** The different HA derivatives were solubilized in 0.01 M HEPES buffer containing
9 0.15 M NaCl pH 7.4. The dissolution time was at least 12 h at 4 °C. The solutions of HA-1,2-
10 BORIN or HA-2,1-BORIN or HA-BOR or HA-PBA and of HA-fructose were mixed under
11 vigorous stirring at room temperature, at a total polymer concentration of 15 g/L and with
12 boronic acid/sugar molar ratio of 1. The mixtures were then allowed to rest at 4 °C overnight
13 before rheological analysis. To study the rheological properties of HA hydrogels as a function of
14 pH, the same buffer was prepared at pH values adjusted to 6, 6.5, 7, 8 and 9.

15 **Rheology.** Oscillatory shear experiments were performed with a cone-plate rheometer
16 (AR2000Ex from TA Instruments). The cone used for viscoelastic samples has a diameter of 2
17 cm and an angle of 4°, whereas viscous solutions were analyzed using a cone of 6 cm of
18 diameter and an angle of 1°. To prevent water evaporation, the measuring system was
19 surrounded with a low-viscosity silicon oil (50 mPa.s) carefully added to the edges of the cone.

1 Oscillatory frequency sweep (0.01-10 Hz) experiments were performed within the linear
2 viscoelastic range (strain fixed at 5 %) to determine the frequency dependence of the storage
3 (G') and loss (G'') moduli. No frequency data beyond 10 Hz are presented because inertial
4 artefacts (raw phase angle $> 150^\circ$) were observed at frequencies higher than 10 Hz.^{31,32}
5 Oscillatory amplitude sweep experiments at 1 Hz were used to determine the linear-viscoelastic
6 range of the hydrogel networks and to derive the yield stress. They were immediately followed
7 by time sweep experiments at 1 Hz and a strain of 5 % (linear viscoelastic region) to monitor the
8 recovery of the rheological moduli. For the measurement of the self-recovery of the gels after
9 four cycles of strain-induced breakdowns, four cycles of a time sweep experiment (strain of 350
10 % at 1 Hz) with a duration of 2 min followed by a time sweep experiment (strain of 5 % at 1 Hz)
11 with a duration of 3 min were performed. The yield stress was determined by steady state stress
12 sweep experiments, consisting in the variation of the viscosity as a function of the shear stress
13 (0.1-1500 Pa) for 15 min.

14 **Injection force measurements.** Hydrogel injection forces were measured using a mechanical
15 testing machine (SHIMADZU EZ-SX). A “homemade” support was used to fix and stabilize the
16 syringe during the test. The measurements were made using the tensile extension mode, at a flow
17 rate of 1 mm/mL. Hydrogels were prepared as previously described and loaded into 1 mL
18 syringes. The loaded syringes were kept at 4 °C overnight before analysis at room temperature.
19 Hydrogel injection forces were measured over time using a 27 G needle.

20 **Determination of K_a by ITC.** Calorimetric titration experiments were carried out on a Microcal
21 VP-ITC titration microcalorimeter (Northampton, U.S.A.). All titrations were performed using
22 solutions of 1,2-ABORIN (2,1-ABORIN or ABOR or APBA) and free D-fructose solubilized in
23 0.01 M PBS, with pH adjusted to 7.4 (± 0.1) using a pH-meter, by carefully adding 1 M NaOH

1 when necessary. The reaction cell ($V = 1.4478$ mL) contained a solution of “molecule 2” (Table
2 2). A series of 28 injections of 5 or 10 μL of a solution of “molecule 1” was made from a
3 computer-controlled 300 μL microsyringe at an interval of 400 s into the solution contained in
4 the reaction cell, while stirring at 300 rpm at 25°C. The raw experimental data were reported as
5 the amount of heat produced after each injection of boronic acid as a function of time. The
6 amount of heat produced per injection was calculated by integration of the area under individual
7 peaks by the instrument software, after taking into account heat of dilution. The data were
8 analyzed using the one set of site fitting model (Origin 7.0 software package). Table 2
9 summarizes the experimental conditions used for the ITC measurements.

10 **Table 2.** Experimental conditions of the calorimetric titrations.

Entry	Molecule 1 in syringe	[Molecule 1] (mM)	Molecule 2 in cell	[Molecule 2] (mM)
1	D-fructose	75	1,2-ABORIN	2
2	D-fructose	125	2,1-ABORIN	3.5
3	D-fructose	175	APBA	5
4	D-fructose	75	ABOR	2

11

12 **3D cell encapsulation and cell viability study.** Mouse embryonic fibroblasts (MEFs) used in
13 this study were isolated from mice from the age of embryonic day 12 to postnatal day 1. Culture
14 of cells was performed as described in detail earlier.³³ Briefly, cells were plated onto TCPS in
15 standard growth media based on low-glucose Dulbecco’s modified Eagle’s medium (DMEM)
16 supplemented with 5% FBS, 1% GlutaMAX (Gibco) and 1% penicillin-streptomycin. Cells were
17 expanded when they reached 70-80 confluency. All experiments were performed using cells at
18 passage 13-16. MEFs were then trypsinized, pelleted and resuspended into growth media for cell
19 counting. An aliquot of growth media containing MEFs were then taken to obtain a final density

1 of encapsulated cells in the hydrogels of 5×10^5 cells/mL. Cells were pelleted and resuspended
2 with a solution of the HA-fructose derivative in PBS. The cell-laden solution of HA-fructose and
3 the HA-1,2-BORIN (PBA) solution were pipetted several times and quickly transferred
4 individually to a syringe barrel. 200 μ L of cell-encapsulated hydrogels were prepared by mixing
5 the two HA components using a double-barrel syringe equipped with an extruder (MEDMIX,
6 Switzerland) and transferred to Transwell[®] cell culture inserts (0.4 μ m porous membrane;
7 Corning[®]) contained in 24-well plates. Cell-laden gels were supplemented with standard growth
8 media and incubated for evaluating cell viability over 7 days (37°C and 5% CO₂). For a control,
9 MEFs were incubated only in growth media at a density of 2×10^4 cells/mL. Further studies of
10 cytotoxicity by a MTT (3-(4,5-dimethylthiazol-2-yl)-2,5-diphenyl tetrazolium bromide) assay of
11 modified polymers was performed as previously described.³⁴ Mouse embryonic fibroblasts
12 (MEFs) were cultured in 96-well plates containing 5000 cells incubated with individual solutions
13 of HA derivatives (HA-1,2-BORIN, HA-PBA, HA-fructose) or native HA at 7.5 g/L in standard
14 growth media. After incubation at 37 °C for 72 h, a MTT solution was added in each well at a
15 final concentration of 0.5 g/L. After 2 h, the incubation media was removed and the blue MTT–
16 formazan product was extracted with DMSO. After 15 min extraction at room temperature, the
17 absorbance of the formazan solution was measured spectrophotometrically at 570 nm. The
18 percentage of living cells was calculated based on values of absorbance measured for cells
19 cultured only in growth media. The experiment was repeated 2 times independently.

20 **Live/Dead assay and image acquisition.** The live/dead assay was performed to determine cell
21 viability using a staining kit (calcein-AM/propidium iodide) purchased from Sigma-Aldrich. The
22 staining solution was made according to supplier information, by adding 10 μ L of the calcein-
23 AM solution (green, excitation/emission 490/515 nm) and 5 μ L of the propidium iodide solution

1 (red, excitation/emission 535/617 nm) in 5 mL PBS. After 7 days of cells incubation in the
2 hydrogels, the cell media was removed and the staining solution was then added to the gels with
3 incubation for 15 minutes at 37 °C. Hydrogels containing labeled MEFs were then analyzed
4 under fluorescence microscope (ZEISS Axio Observer 7 ApoTome.2). 2D images were captured
5 from 4 random fields of view for each sample. Fluorescently labeled cells in green (live cells)
6 and red (dead cells) were counted using Image analysis software, ImageJ. Furthermore, 3D
7 images were taken using a laser scanning confocal microscope (Nikon, LSM710) equipped with
8 a high-speed 97-actuator deformable mirror (DM) (AlpAO) for aberration correction.³⁵ Images
9 of cells encapsulated in 3D in the hydrogels (acquisition through encapsulated hydrogels in
10 Transwell[®] cell culture inserts) were acquired using a Nikon 40× (NA = 1.15) water objective.
11 Three-dimensional views were first reconstructed from z-stack images (step size 1 μm) using
12 NIS-Element AR software (Nikon). Living cells stained with calcein-AM (green) were
13 determined from the FITC channel.

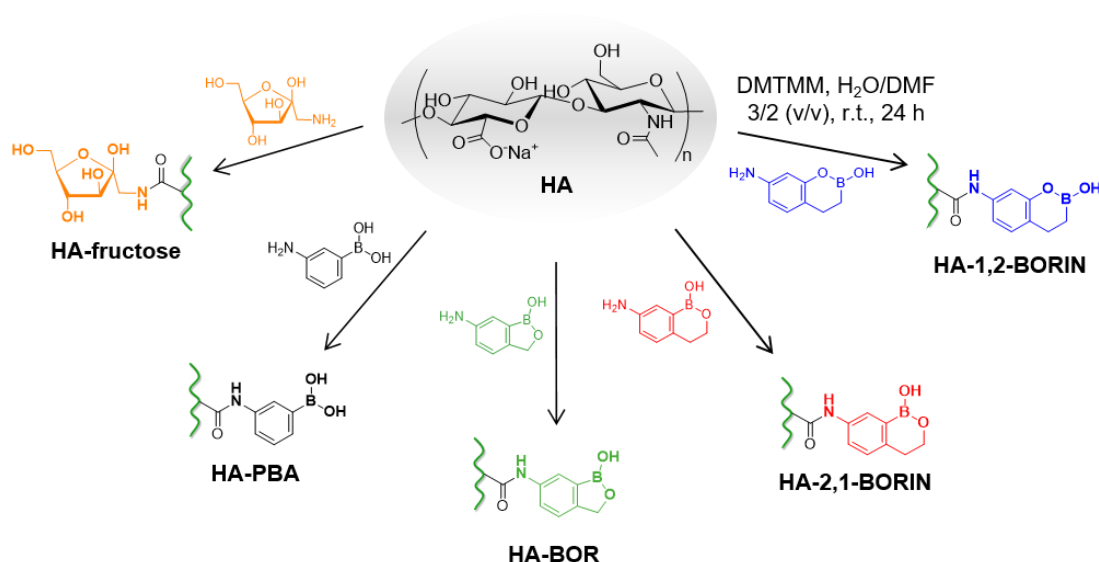
14

15 **Results**

16 To properly investigate the effect of the different small molecule crosslinkers on the
17 rheological properties of the HA networks, all HA derivatives were synthesized from the same
18 HA sample, possessing a weight-average molar mass (M_w) of 360 kg/mol (referred to as
19 HA360), and with a similar degree of substitution (DS, average number of substituting group per
20 repeating disaccharide unit). The synthesis of HA-benzoxaborin conjugates required first that of
21 aminobenzoxaborin derivatives (1,2-ABORIN and 2,1-ABORIN, Figure 2). These custom-made
22 products were synthesized in four- to seven-steps, as described in the Supporting Information,

1 and were isolated with yields comprised between 81 and 82 %. The HA-1,2-BORIN, HA-2,1-
2 BORIN, HA-BOR, HA-PBA and HA-fructose conjugates were prepared by an amide coupling
3 reaction carried out in aqueous solution between 3,4-dihydro-2H-benzo[e][1,2]oxaborinin-2-ol
4 (1,2-ABORIN), 3,4-dihydro-1H-benzo[c][1,2]oxaborinin-1-ol (2,1-ABORIN), 6-
5 aminobenzoxaborole (ABOR), 3-aminophenylboronic acid (APBA) and 1-amino-1-deoxy-D-
6 fructose (fructosamine), respectively, and HA, using 4-(4,6-dimethoxy-1,3,5-triazin-2-yl)-4-
7 methylmorpholinium chloride (DMTMM) as a coupling agent (Figure 2).³⁶ The DS of the HA
8 conjugates was controlled by the amount of amine to carboxylic acid. Using DMTMM/HA and
9 amine/HA molar ratios of 1 and 0.15, respectively, we obtained HA derivatives with a DS of 0.1-
10 0.15 from ¹H NMR analysis (Figure S1-S4). In the case of HA-fructose, successful grafting was
11 confirmed by 2D HSQC NMR analysis (Figure S5), and a DS of 0.15 was estimated from the
12 reaction kinetics performed using 2,4,6-trinitrobenzene sulfonic acid (TNBS) to quantify the free
13 primary amines in the reaction medium as a function of time (Figure S6).³⁷

14

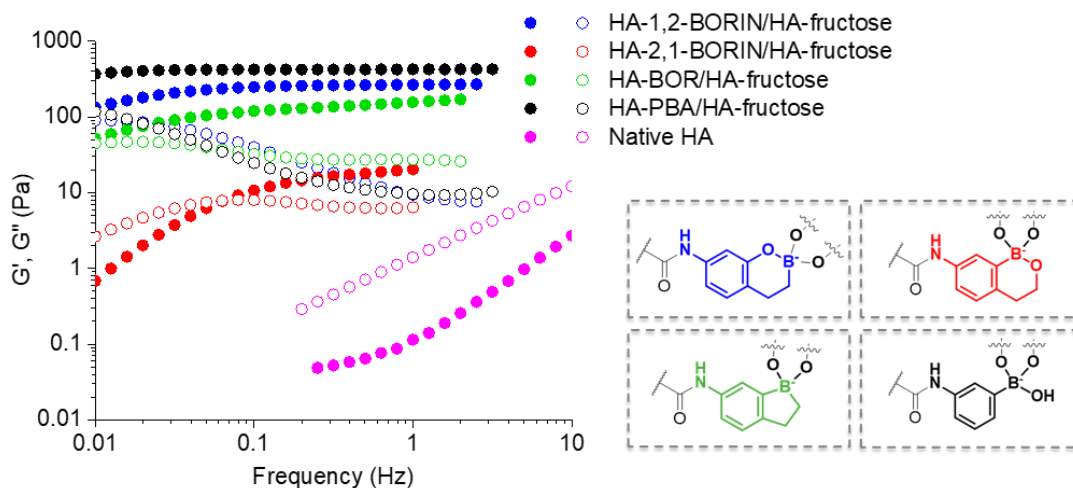


15

1 **Figure 2.** Synthetic scheme for the preparation of HA derivatives via amide coupling reaction.

2 The different HA-based networks were then produced by mixing thoroughly aqueous
3 solutions of HA-1,2-BORIN (or HA-2,1-BORIN or HA-BOR or HA-PBA) and HA-fructose at
4 physiological pH (0.01 M HEPES buffer, 0.15 M NaCl), at a total polymer concentration ($C_p =$
5 15 g/L) higher than the overlap concentration of initial HA360 ($C^* \approx 1$ g/L), and with a molar
6 ratio of 1,2-BORIN (2,1-BORIN or BOR or PBA)-to-grafted fructose of 1. Dynamic rheological
7 analyses revealed a gel-like behavior ($G' > G''$) within the frequency window explored for the
8 mixtures based on HA-1,2-BORIN (PBA) (BOR) and HA-fructose (Figure 3). A comparison
9 between these three formulations showed that the elastic modulus at the plateau region is higher
10 for the HA-PBA/HA-fructose assembly ($G'_{\text{plateau}} = 424$ Pa), than for the HA-1,2-BORIN/HA-
11 fructose and HA-BOR/HA-fructose networks ($G'_{\text{plateau}} = 266$ Pa and 156 Pa, respectively). A
12 larger discrepancy between G' and G'' was also observed for the HA-PBA/HA-fructose mixture,
13 indicating a higher resistance to flow. By contrast, the assembly based on HA-2,1-BORIN
14 showed a viscoelastic behavior (crossover of G' and G'' seen within the tested frequencies) with
15 a G' value at the plateau region of 20 Pa.

16

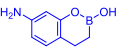
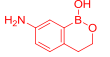
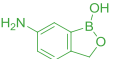
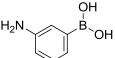


1
 2 **Figure 3.** Dynamic rheological behavior of HA networks (M_w HA = 360 kg/mol) based on
 3 boronic acid/fructose crosslinks. Frequency dependence of the storage modulus (G' , filled
 4 symbols) and loss modulus (G'' , empty symbols) of formulations based on HA-fructose mixed
 5 with HA-1,2-BORIN or HA-2,1-BORIN or HA-BOR or HA-PBA at pH 7.4 (1,2-BORIN or 2,1-
 6 BORIN or BOR or PBA/fructose molar ratio of 1).

7 On the basis of these observations, we investigated the relationships between the
 8 macroscopic mechanical properties and the small molecule crosslinkers by analyzing the
 9 thermodynamics of boronic acid-fructose complexation. As the bound and unbound forms of
 10 these boronic acid derivatives in the presence of fructose are distinguishable by ^1H NMR
 11 spectroscopy,^{15,38} we used this technique to measure their affinities for free/grafted fructose
 12 (Table 3, Figure S7-S14). The values of K_a for free D-fructose were also examined by isothermal
 13 titration calorimetry (ITC) and were in the same order of magnitude as the values derived from
 14 ^1H NMR (Table 3, Figure S15-S18).

15

1 **Table 3.** Binding constants of complexes based on 1,2-ABORIN (2,1-ABORIN or ABOR or
 2 APBA) with free D-fructose or grafted fructose (HA-fructose).

Entry	Derivative	Saccharide	$K_a^{a)}$ NMR (M^{-1})	$K_a^{b)}$ ITC (M^{-1})	$n^{b)}$ (n saccharide : 1 boronic acid)	$\Delta H^{b)}$ (kJ/mol)	$\Delta S^{b)}$ (J.mol/K)
1	1,2- ABORIN	D-fructose	487 ± 49	531 ± 40	1.07 ± 0.05	-10.3 ± 0.6	18
	 HA-fructose	$-^c)$					
2	2,1- ABORIN	D-fructose	87 ± 13	74 ± 17	n fixed at 1 ^{d)}	-16.7 ± 0.4	-20
	 HA-fructose	179 ± 67					
3	ABOR	D-fructose	461 ± 73	484 ± 50	1.24 ± 0.1	-11.7 ± 1.2	12.1
	 HA-fructose	545 ± 28					
4	APBA	D-fructose	201 ± 5	112 ± 16	1.3 ± 0.3	-11.2 ± 2.8	1.6
	 HA-fructose	503 ± 18					

3 ^{a)}Measured from at least two ¹H NMR experiments; ^{b)}measured from at least two ITC
 4 experiments; ^{c)}not determined because the bound and unbound forms of 1,2-ABORIN are not
 5 sufficiently separated to be properly integrated; ^{d)}calorimetric curve fitting by applying a fixed
 6 value of $n = 1$.

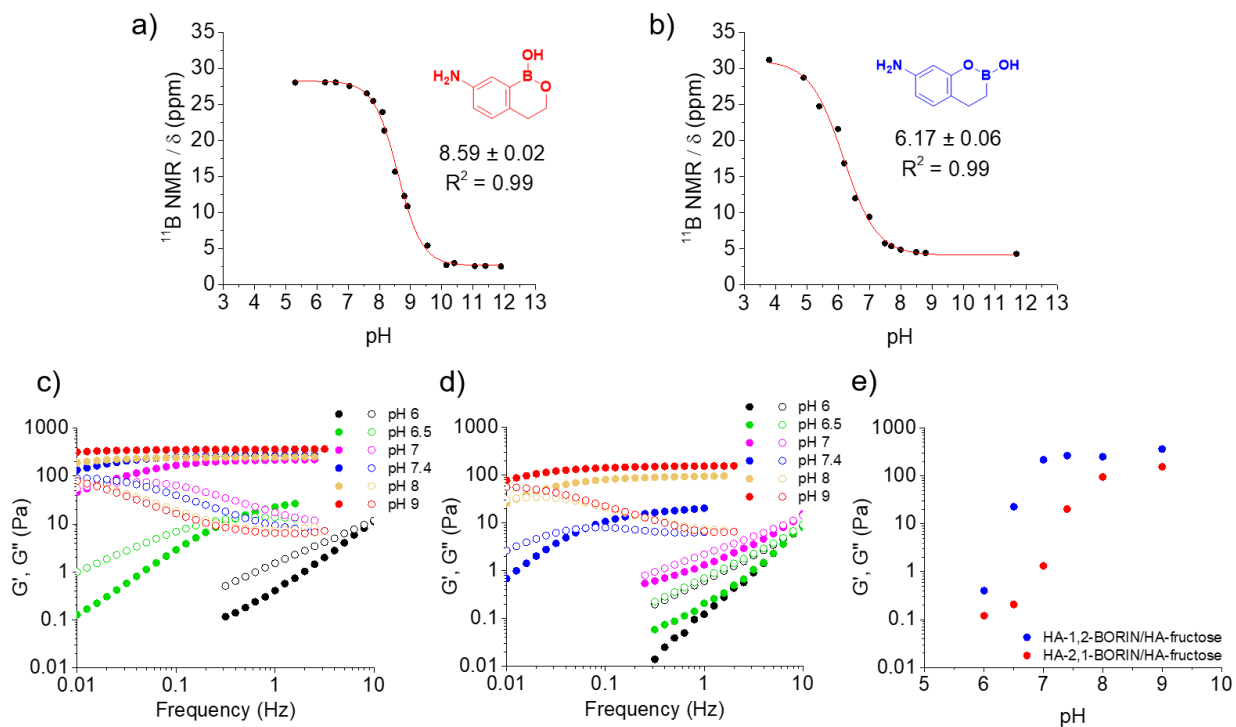
7 From Table 3, we observe that relatively close values of K_a (in the same order of
 8 magnitude) were determined for 1,2-ABORIN (ABOR) with free and grafted fructose as well as
 9 for APBA with grafted fructose (Table 3, entries 1, 3 and 4). These results are consistent with the
 10 gel-like behavior observed for the HA mixtures based on these derivatives (Figure 3). Regarding
 11 complexation with APBA, a 2-fold increase of K_a was observed for HA-fructose compared to D-
 12 fructose (Table 3, entry 4). Moreover, despite the close values of K_a found for the complexation
 13 of APBA (ABOR) with fructose grafted on HA, a lower elastic modulus was measured for the

1 HA-BOR/HA-fructose mixture. This may be ascribed to competitive interactions between BOR
2 and HA saccharides as demonstrated by steady shear flow and dynamic rheological experiments
3 performed on HA-BOR alone and initial (native) HA360 at pH 7.4 (Figure S19). Indeed, these
4 measurements showed that HA-BOR stands out among the other HA derivatives (HA-1,2-
5 BORIN HA-2,1-BORIN and HA-PBA) by giving rise to solutions with higher dynamic moduli
6 and viscosity compared to native HA360 (Figure S19). Moreover, ^1H NMR analysis of this
7 derivative at neutral pH provided another evidence of the selective binding of benzoboroxole
8 moieties to HA. This indeed showed additional ^1H signals in the aromatic region of grafted BOR
9 moieties, suggesting the presence of free and complexed BOR species which are in slow
10 exchange on the NMR timescale (Figure S3). Regarding the interaction of 2,1-ABORIN with
11 free/grafted fructose, the low K_a measured for these couples in comparison to the other pairs
12 correlates with the low G' value at the plateau and faster dynamics of the HA-2,1-BORIN/HA-
13 fructose mixture (Table 3, entry 2).

14 Taken together, these results demonstrate that the macroscopic rheological behavior of the
15 HA assemblies are closely related to the binding affinities of their small molecular crosslinkers.
16 Considering that all mixtures only differ in the nature of their boronic acid partner, the binding
17 mechanism allowing boronate ester formation may strongly depend on the structure and physico-
18 chemical properties of each derivative used. In these systems, one determinant factor that may
19 affect K_a and boronate crosslinking formation is the $\text{p}K_a$ of the boronic acid group. Surprisingly,
20 in the case of complexation between APBA (ABOR) and HA-fructose, boronate esters were
21 formed with similar affinities in spite of their different structures and values of $\text{p}K_a$ (8.8 for
22 PBA²³ and 7.3 for BOR¹⁴). On the other hand, regarding the 2,1-ABORIN derivative, the weak
23 interaction with fructose may be partially related to its relatively high $\text{p}K_a$ (8.59, Figure 4a),

1 which is due to its structure containing a less strained six-membered heterocycle compared to
2 benzoboroxole.¹⁴ By contrast, the disposition of the endocyclic B-O bond in 1,2-ABORIN, with
3 the oxygen atom between the phenyl ring and boron, suggests a more electron-deficient character
4 of the boronic center and, therefore, a higher acidity. Indeed, a pK_a value of 6.17 was determined
5 for free 1,2-ABORIN by ¹¹B NMR titration^{15,25} (Figure 4b). Interestingly, the dynamic
6 rheological properties of the HA-1,2-BORIN (HA-2,1-BORIN)/HA-fructose networks at a pH
7 range of 6-9 are consistent with the values of pK_a measured for the free derivatives. As
8 demonstrated in Figure 4c, formation of crosslinks in the HA-1,2-BORIN/HA-fructose system
9 was observed in this pH range. This assembly showed a remarkable increase of the elastic
10 modulus at pH 7 and a gel-like behavior from pH 7.4. By contrast, crosslinking in HA-2,1-
11 BORIN/HA-fructose was effective only from pH 7.4, and a pH value around 9 is required to
12 achieve a gel-like behavior (Figure 4d). The higher cross-linking efficiency of HA-1,2-
13 BORIN/HA-fructose at physiological pH can be related to the lower pK_a of 1,2-ABORIN, than
14 that of 2,1-ABORIN (Figure 4e). Collectively, these results indicate that the contrasting acidities
15 of these benzoxaborin compounds are a main factor determining the different rheological
16 properties of the HA mixtures.

17



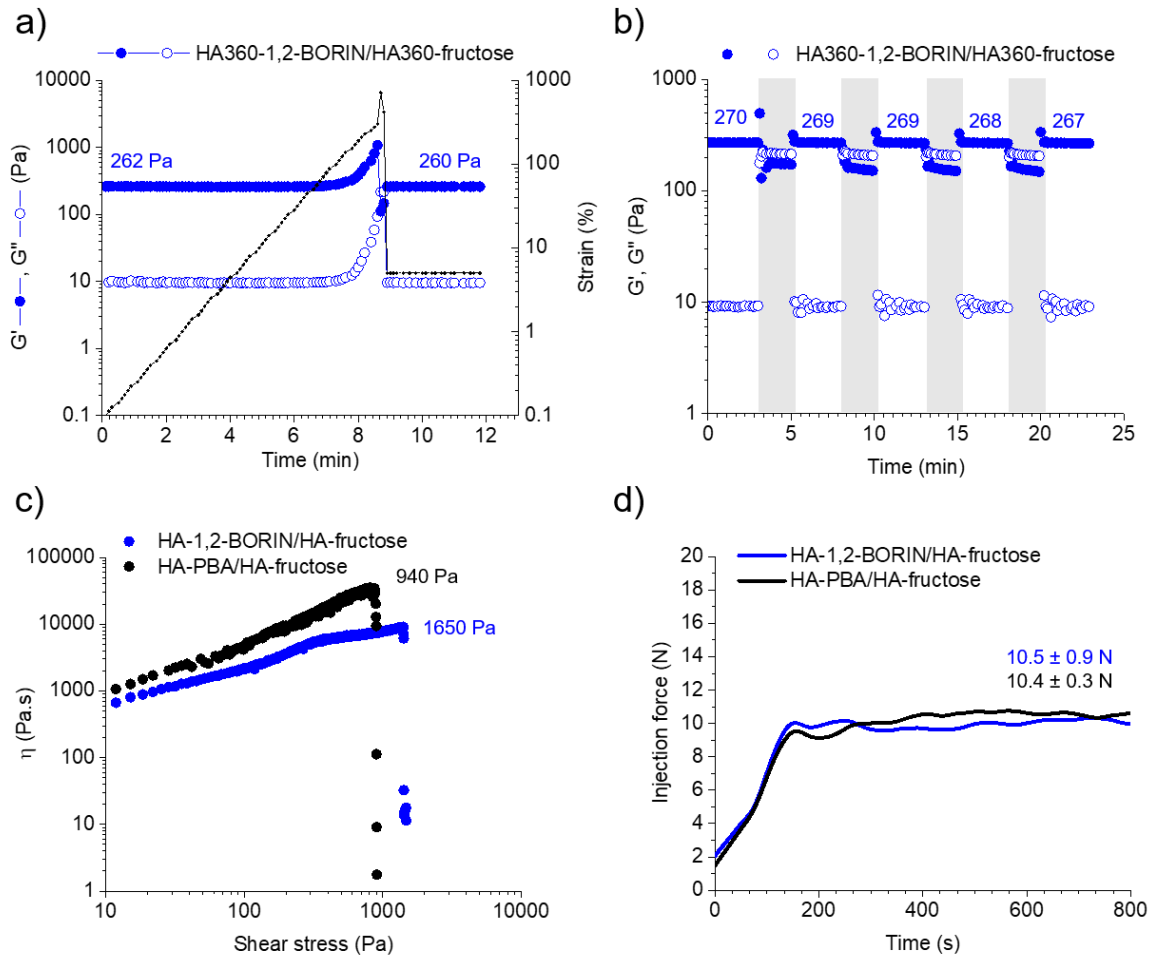
1
 2 **Figure 4.** Values of pK_a determined for (a) free 2,1-BORIN and (b) free 1,2-BORIN by ^{11}B
 3 NMR spectroscopy. Dynamic rheological properties of the HA-1,2-BORIN (2,1-BORIN)/HA-
 4 fructose networks by varying the pH of the medium from 6 to 9: frequency dependence of G'
 5 (filled symbols) and G'' (empty symbols) of (c) HA-1,2-BORIN/HA-fructose and (d) HA-2,1-
 6 BORIN/HA-fructose; (e) variation of G' at a frequency of 1 Hz as a function of pH for the
 7 mixtures based on HA-fructose and HA-1,2-BORIN (2,1-BORIN).

8 On the basis of these results, the HA-1,2-BORIN/HA-fructose network, exhibiting slow
 9 relaxing properties at physiological pH, was considered more suitable as injectable cell carrier
 10 for regenerative medicine and tissue engineering applications. Therefore, in the next step, we
 11 investigated its self-healing and injectability properties in comparison to the HA-PBA/HA-
 12 fructose hydrogel. The latter network was selected as a reference as some limitations were found
 13 when using the HA-BOR/HA-fructose assembly due to the increased rheological moduli and

1 viscosity of the HA-BOR solution, as previously discussed, which caused difficulties to prepare
2 the HA-BOR/HA-fructose gel homogeneously loaded with cells for 3D cell culture experiments.

3 As shown in Figure 5a, strain-dependent oscillatory measurements displayed a broad linear
4 viscoelastic region with network failure at high strain (700 %). The network was then found to
5 immediately recover its rheological properties when the strain was reduced to 5 %. Then, the gel
6 was exposed to a series of four cycles of breaking and reforming, which consisted in applying
7 high strains (350 %) for 3 min, intercalated with low strains (5 %) for 2 min (Figure 5b). After
8 this series of four cycles, the hydrogel was able to recover its initial rheological moduli,
9 demonstrating its self-healing property. Although dynamic rheological moduli and self-healing
10 capacity are important parameters for determining injectability, quantification of the viscosity
11 and yield stress,³⁹ as well as the injection force required to extrude a gel through a needle, are
12 also important to determine whether or not it is relevant for injection uses.⁴⁰ Therefore, we
13 evaluated the yield stress and viscosity of the new HA-1,2-BORIN/HA-fructose hydrogel in
14 comparison to the HA assembly based on HA-PBA/HA-fructose. The yield stress is defined as
15 the stress at which the network starts to flow, indicated as the first read-out of viscosity on the
16 rheometer. As illustrated in Figure 5c, the viscosity of both HA assemblies increased with
17 increasing shear stress. As expected, a higher viscosity was observed for the HA-PBA/HA-
18 fructose hydrogel (η_{\max} of approximately 30000 Pa.s) compared to the HA-1,2-BORIN/HA-
19 fructose networks (η_{\max} of 8000 Pa.s). The yield stress for these formulations were found to be
20 940 and 1650 Pa, respectively. Moreover, values of injection force close to 10 N were required
21 to extrude HA-1,2-BORIN (PBA)/HA-fructose from a 1 mL plastic syringe with a 27 G needle at
22 a flow rate of 1 mm/min (Figure 5d). Despite the fact that the injection force of a gel depends on
23 several factors such as flow rate, needle gauge and needle length, clinically relevant values are

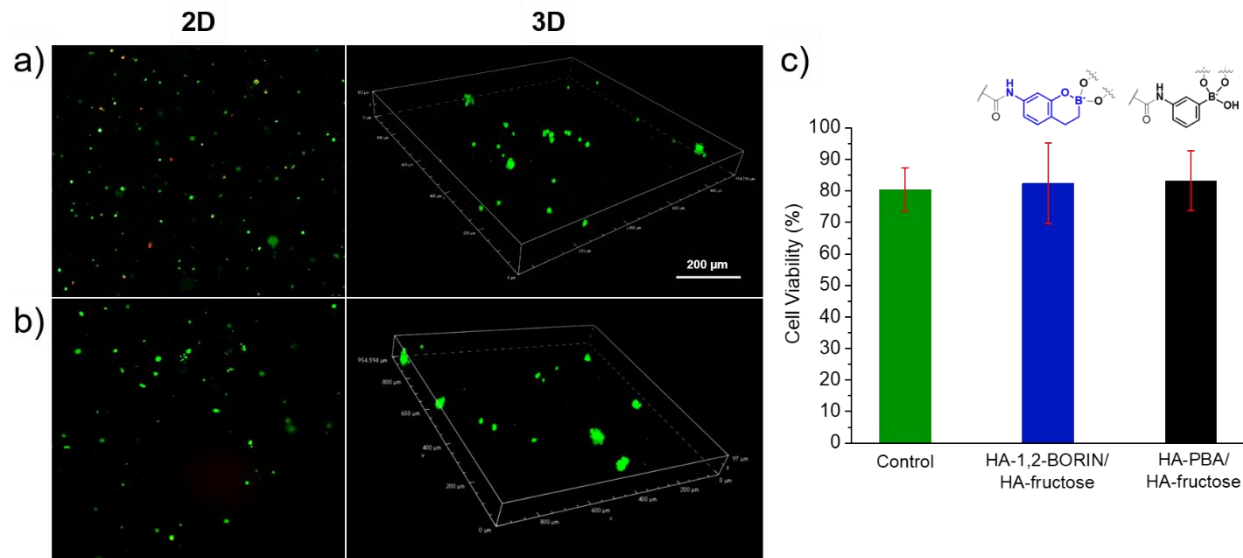
1 often below 20 N.⁴⁰ These experiments thus indicate that both networks are promising candidates
 2 as injectable scaffolds for regenerative medicine and tissue engineering.



3
 4 **Figure 5.** Self-healing ability of the new HA-1,2-BORIN/HA-fructose gel: (a) dynamic
 5 rheological behavior of G' (filled symbols) and G'' (empty symbols) at failure under increasing
 6 strain application (approximately 700 %), followed by the immediate recovery of the rheological
 7 moduli at a strain of 5 % (linear viscoelastic region); and (b) self-recovery of the gel after four
 8 cycles of strain-induced breakdowns, by applying a value of strain above the linear viscoelastic
 9 region (shaded regions, 350 %) for 2 min, followed by linear recovery measurements for 3 min
 10 (unshaded regions, strain of 5 %). Injectability of the HA-1,2-BORIN/HA-fructose hydrogel

1 compared to the HA-PBA/HA-fructose assembly: (c) yield stress and viscosity of both
2 assemblies (average values of yield stress from at least two identical measurements); and (d)
3 injection force measurements over time for both formulations injected from a 1 mL syringe) with
4 a 27 G needle, at a flow rate of 1 mm/min (average values of extrusion force determined from
5 triplicates).

6 Next, we examined the potential of these hydrogels for cell encapsulation by simply
7 mixing solutions of HA-1,2-BORIN (PBA) and HA-fructose loaded with mouse embryonic
8 fibroblasts (MEFs). In these experiments, cells were encapsulated in the HA-1,2-BORIN
9 (PBA)/HA-fructose hydrogels at a density of 5×10^5 cells/mL and cultured in growth media for 7
10 days (37 °C, 5 % CO₂). For a control, MEFs were incubated only in growth media at a density of
11 2×10^4 cells/mL. Thanks to the quasi-instantaneous gelation of the HA-1,2-BORIN (PBA)/HA-
12 fructose mixtures, the cells could be homogeneously distributed in 3D in the two hydrogels. A
13 live/dead assay was used to quantify the live (green) and dead (red) cells by fluorescence and
14 laser scanning confocal microscopy imaging of three-dimensionally encapsulated MEFs in the
15 gel structure (Figure 6a and 6b). The two HA assemblies showed high cytocompatibility over the
16 course of 7 days of cell culture (> 80 % of cell viability, Figure 6c). These data correlate with the
17 low cytotoxicity of individual solutions of HA derivatives, as assessed by a MTT assay including
18 incubation of HA-BORIN, HA-PBA and HA-fructose (solutions at 7.5 g/L) with MEFs for 72 h
19 at 37 °C. This revealed a cell viability > 80 % for the HA-PBA and HA-fructose conjugates,
20 whereas 75 % of viable cells were observed after incubation with HA-1,2-BORIN (Figure S20).
21 Together, these results reveal not only the ability of our HA hydrogels to encapsulate cells in 3D,
22 but also to provide a microenvironment conducive to maintaining cellular function over one
23 week.



1
2 **Figure 6.** Cytocompatibility of boronate-ester crosslinked HA hydrogels after 7 days of 3D cell
3 culture. 2D (fluorescence, scale bar = 500 μm) and 3D (laser scanning confocal, scale bar = 200
4 μm) microscopy images for the live/dead cell assay of mouse embryonic fibroblasts (MEFs)
5 encapsulated in the (a) HA-1,2-BORIN/HA-fructose and (b) HA-PBA/HA-fructose hydrogels at
6 day 7. Cells were stained with calcein AM (green, live) and ethidium homodimer (red, dead). (c)
7 Quantification of cellular viability ($n = 3$). Error bars represent the standard errors of the mean
8 (S.E.M.).

9

10 Conclusion

11 In this work, we demonstrated the feasibility of HA hydrogel formation at physiological
12 pH through complexation of an original benzoxaborin derivative (1,2-BORIN) grafted on HA
13 with a second HA conjugate modified by fructose moieties. This new hydrogel exhibited
14 rheological properties similar to the HA networks obtained by combining classical PBA- or
15 BOR-modified HA and HA-fructose. By contrast, the use of HA functionalized with

1 conventional benzoxaborin (2,1-BORIN) as a boronic acid partner of HA-fructose only allowed
2 formation of a viscoelastic solution with a low elastic modulus. The different macroscopic
3 rheological properties observed for the mixtures based on HA-1,2-BORIN (2,1-BORIN) and
4 HA-fructose were found to be closely linked to the different structures and pK_a values of these
5 boronic acid derivatives. Indeed, the former showed polymer association at lower pH correlating
6 with the low pK_a of free 1,2-ABORIN, whereas the latter exhibited viscoelastic properties only at
7 basic pH due to its higher pK_a . Besides, these original materials showed injectable and self-
8 healing properties together with a high cell viability as demonstrated by 3D cell encapsulation
9 for several days. Continued investigation of the applicability of these HA hydrogels as promising
10 injectable scaffolds for encapsulation of cells or bioactive molecules will expand their
11 application in many innovative biomedical fields.

12 ASSOCIATED CONTENT

13 **Supporting Information.**

14 The Supporting Information is available free of charge on the ACS Publications website.

15 Synthesis of aminobenzoxaborin (ABORIN) compounds; ^1H NMR spectra of HA-1,2-BORIN,
16 HA-2,1-BORIN, HA-BOR and HA-PBA derivatives synthesized by amide coupling reaction
17 (M_w HA = 360 kg/mol); 2D HSQC NMR characterization of HA-fructose conjugate synthesized
18 by amide coupling reaction (M_w HA = 360 kg/mol); determination of the degree of substitution
19 (DS) of HA-fructose from the kinetics of the amide coupling reaction (M_w HA = 360 kg/mol);
20 methodology for K_a measurements by ^1H NMR spectroscopy; determination of K_a by ^1H NMR
21 for 1,2-ABORIN (2,1-ABORIN) and fructose (free fructose and HA-fructose); determination of
22 K_a by ^1H NMR for APBA (ABOR) and fructose (free fructose and HA-fructose); calorimetric
23 titration of 1,2-ABORIN (2,1-ABORIN) with free D-fructose; calorimetric titration of APBA

1 (ABOR) with free D-fructose; rheological analysis of the HA-1,2-BORIN (2,1-BORIN, BOR or
2 PBA) alone at pH 7.4 (M_w HA = 360 g/mol); cytotoxicity (MTT) assay of individual solutions of
3 HA derivatives incubated with mouse embryonic fibroblasts (MEFs).

4

5 AUTHOR INFORMATION

6 **Corresponding Author**

7 * E-mail: rachel.auzely@cermav.cnrs.fr

8 **Author Contributions**

9 The manuscript was written through contributions of all authors. All authors have given approval
10 to the final version of the manuscript.

11 ACKNOWLEDGMENT

12 This work was supported by Galderma-Nestlé Skin Health. The authors thank Dr. C. Bouix-Peter
13 at Galderma R&D for valuable discussions; Bellen Chemistry and GVK Biosciences for the
14 custom synthesis of aminobenzoxaborin derivatives; the NMR platform of ICMG (FR2607) for
15 its support; and Dr. Alexei Grichine, Dr. Antoine Delon and Tom Delaire from the IAB
16 microscopy platform (Grenoble) for the confocal imaging of fibroblasts cells cultured in our
17 hydrogels.

18 REFERENCES

19 (1) Brochu, A. B. W.; Craig, S. L.; Reichert, W. M. Self-healing Biomaterials. *Journal of*
20 *Biomedical Materials Research A* **2011**, *96* (2), 492-506.

21 (2) Taylor, D. L.; Panhuis, M. in het. Self-healing Hydrogels. *Adv. Mater.* **2016**, *28*, 9060–
22 9093.

- 1 (3) Zhang, L.; Tian, M.; Wu, J. Hydrogels with Self-Healing Attribute. In *Emerging Concepts*
2 *in Analysis and Applications of Hydrogels*; Majee, S. B. Ed. IntechOpen: **2016**, p. 231.
- 3 (4) Loebel, C.; Rodell, C. B.; Chen, M. H.; Burdick, J. A. Shear-Thinning and Self-Healing
4 Hydrogels as Injectable Therapeutics and for 3D-Printing. *Nat. Protoc.* **2017**, *12* (8), 1521–1541.
- 5 (5) Wei, Z.; Yang, J. H.; Zhou, J.; Xu, F.; Zrínyi, M.; Dussault, P. H.; Osada, Y.; Chen, Y. M.
6 Self-Healing Gels Based on Constitutional Dynamic Chemistry and Their Potential Applications.
7 *Chem Soc Rev* **2014**, *43* (23), 8114–8131.
- 8 (6) Tang, S.; Ma, H.; Tu, H.-C.; Wang, H.-R.; Lin, P.-C.; Anseth, K. S. Adaptable Fast
9 Relaxing Boronate-Based Hydrogels for Probing Cell-Matrix Interactions. *Adv. Sci.* **2018**, *5*,
10 1800638.
- 11 (7) Wang, Y.; Li, L.; Kotsuchibashi, Y.; Vshyvenko, S.; Liu, Y.; Hall, D.; Zeng, H.; Narain R.
12 Self-Healing and Injectable Shear Thinning Hydrogels Based on Dynamic Oxaborole-Diol
13 Covalent Cross-Linking. *ACS Biomater. Sci. Eng.* **2016**, *2*, 2315–2323.
- 14 (8) Wu, D.; Wang, W.; Diaz-Dussan, D. Peng, Y.-Y.; Chen, Y.; Narain, R.; Hall, D. G. In Situ
15 Forming, Dual-Crosslink Network, Self-Healing Hydrogel Enabled by a Bioorthogonal
16 Nopoldiol–Benzoxaborolate Click Reaction with a Wide pH Range. *Chem. Mater.* **2019**, *31*,
17 4092–4102.
- 18 (9) Yesilyurt, V.; Webber, M. J.; Appel, E. A.; Godwin, C.; Langer, R.; Anderson, D. G.
19 Injectable Self-Healing Glucose-Responsive Hydrogels with PH-Regulated Mechanical
20 Properties. *Adv. Mater.* **2016**, *28* (1), 86–91.
- 21 (10) Yan, J.; Springsteen, G.; Deeter, S.; Wang, B. The Relationship among pKa, pH, and
22 Binding Constants in the Interactions between Boronic Acids and Diols—It Is Not as Simple as
23 It Appears. *Tetrahedron* **2004**, *60* (49), 11205–11209.
- 24 (11) Lin, M.; Sun, P.; Chen, G.; Jiang, M. The Glyco-Stereoisomerism Effect on Hydrogelation
25 of Polymers Interacting via Dynamic Covalent Bonds. *Chem Commun* **2014**, *50* (68), 9779–
26 9782.
- 27 (12) Mulla, H. R.; Agard, N. J.; Basu, A. 3-Methoxycarbonyl-5-Nitrophenyl Boronic Acid:
28 High Affinity Diol Recognition at Neutral pH. *Bioorg. Med. Chem. Lett.* **2004**, *14* (1), 25–27.
- 29 (13) Zhang, C.; Losego, M. D.; Braun, P. V. Hydrogel-Based Glucose Sensors: Effects of
30 Phenylboronic Acid Chemical Structure on Response. *Chem. Mater.* **2013**, *25* (15), 3239–3250.
- 31 (14) Tomsho, J. W.; Pal, A.; Hall, D. G.; Benkovic, S. J. Ring Structure and Aromatic
32 Substituent Effects on the pKa of the Benzoxaborole Pharmacophore. *ACS Med. Chem. Lett.*
33 **2012**, *3* (1), 48–52.
- 34 (15) Dowlut, M.; Hall, D. G. An Improved Class of Sugar-Binding Boronic Acids, Soluble and
35 Capable of Complexing Glycosides in Neutral Water. *J. Am. Chem. Soc.* **2006**, *128* (13), 4226–
36 4227.

- 1 (16) Adamczyk-Woźniak, A.; Borys, K. M.; Sporzyński, A. Recent Developments in the
2 Chemistry and Biological Applications of Benzoxaboroles. *Chem. Rev.* **2015**, *115*, 5224–5247.
- 3 (17) Dong, Y.; Wang, W.; Veiseh, O.; Appel, E. A.; Xue, K.; Webber, M. J.; Tang, B. C.;
4 Yang, X.-W.; Weir, G. C.; Langer, R.; Anderson, D. G. Injectable and Glucose-Responsive
5 Hydrogels Based on Boronic Acid–Glucose Complexation. *Langmuir* **2016**, *32* (34), 8743–8747.
- 6 (18) Roberts, M. C.; Hanson, M. C.; Massey, A. P.; Karren, E. A.; Kiser, P. F. Dynamically
7 Restructuring Hydrogel Networks Formed with Reversible Covalent Crosslinks. *Adv. Mater.*
8 **2007**, *19* (18), 2503–2507.
- 9 (19) Tarus, D.; Hachet, E.; Messenger, L.; Catargi, B.; Ravaine, V.; Auzély-Velty, R. Readily
10 Prepared Dynamic Hydrogels by Combining Phenyl Boronic Acid- and Maltose-Modified
11 Anionic Polysaccharides at Neutral PH. *Macromol. Rapid Commun.* **2014**, *35* (24), 2089–2095.
- 12 (20) Deng, C. C.; Brooks, W. L. A.; Abboud, K. A.; Sumerlin, B. S. Boronic Acid-Based
13 Hydrogels Undergo Self-Healing at Neutral and Acidic pH. *ACS Macro Lett.* **2015**, *4* (2), 220–
14 224.
- 15 (21) Chen, Y.; Wang, W.; Wu, D.; Nagao, M.; Hall, D. G.; Thundat, T.; Narain, R. Injectable
16 Self-Healing Zwitterionic Hydrogels Based on Dynamic Benzoxaborole–Sugar Interactions with
17 Tunable Mechanical Properties. *Biomacromolecules* **2018**, *19* (2), 596–605.
- 18 (22) Chen, Y.; Diaz-Dussan, D.; Wu, D.; Wang, W.; Peng, Y.-Y.; Asha, A. B.; Hall, D. G.;
19 Ishihara, K.; Narain, R. Bioinspired Self-Healing Hydrogel Based on Benzoxaborole-Catechol
20 Dynamic Covalent Chemistry for 3D Cell Encapsulation. *ACS Macro Lett.* **2018**, *7* (8), 904–908.
- 21 (23) Springsteen, G.; Wang, B. A Detailed Examination of Boronic Acid–Diol Complexation.
22 *Tetrahedron* **2002**, *58* (26), 5291–5300.
- 23 (24) Liu, C. T.; Tomsho, J. W.; Benkovic, S. J. The Unique Chemistry of Benzoxaboroles:
24 Current and Emerging Applications in Biotechnology and Therapeutic Treatments. *Bioorg. Med.*
25 *Chem.* **2014**, *22* (16), 4462–4473.
- 26 (25) Bérubé, M.; Dowlut, M.; Hall, D. G. Benzoboroxoles as Efficient Glycopyranoside-
27 Binding Agents in Physiological Conditions: Structure and Selectivity of Complex Formation. *J.*
28 *Org. Chem.* **2008**, *73* (17), 6471–6479.
- 29 (26) Sumida, Y.; Harada, R.; Kato-Sumida, T.; Johmoto, K.; Uekusa, H.; Hosoya, T. Boron-
30 Selective Biaryl Coupling Approach to Versatile Dibenzoxaborins and Application to Concise
31 Synthesis of Defucogilvocarcin M. *Org. Lett.* **2014**, *16* (23), 6240–6243.
- 32 (27) Saito, H.; Otsuka, S.; Nogi, K.; Yorimitsu, H. Nickel-Catalyzed Boron Insertion into the
33 C2–O Bond of Benzofurans. *J. Am. Chem. Soc.* **2016**, *138* (47), 15315–15318.
- 34 (28) Angyal, S. J. The Composition of Reducing Sugars in Solution. In *Advances in*
35 *Carbohydrate Chemistry and Biochemistry*; Tipson, R. S., Horton, D., Eds.; Academic Press,
36 **1984**; Vol. 42, pp 15–68.

- 1 (29) Wu, X.; Li, Z.; Chen, X.-X.; Fossey, J. S.; James, T. D.; Jiang, Y.-B. Selective Sensing of
2 Saccharides Using Simple Boronic Acids and Their Aggregates. *Chem. Soc. Rev.* **2013**, *42* (20),
3 8032.
- 4 (30) Macosko, C. W. G. *Rheology: Principles, Measurements, and Applications*; VCH
5 Publishers: Weinheim, Germany, **1994**.
- 6 (31) Krieger, I. M. The Role of Instrument Inertia in Controlled-Stress rheometers. *J. Rheol.*
7 **1990**, *34* (4), 471–483.
- 8 (32) Hudson, R. E.; Holder, A. J.; Hawkins, K. M.; Williams, P. R.; Curtis, D. J. An Enhanced
9 Rheometer Inertia Correction Procedure (ERIC) for the Study of Gelling Systems Using
10 Combined Motor-Transducer Rheometers. *Phys. Fluids* **2017**, *29*, 121602.
- 11 (33) Petropoulos, C.; Oddou, C.; Emadali, A.; Hiriart-Bryant, E.; Boyault, C.; Faurobert, E.;
12 Pol, S. V.; Kim-Kaneyama, J.; Kraut, A.; Coute, Y.; Block, M.; Albiges-Rizo, C.; Destaing, O.
13 Roles of paxillin family members in adhesion and ECM degradation coupling at invadosomes. *J.*
14 *Cell Biol.* **2016**, *213* (5), 585–599.
- 15 (34) Mosmann T. Rapid Colorimetric Assay for Cellular Growth and Survival: Application to
16 Proliferation and Cytotoxicity Assays. *J. Immunol. Methods.* **1983**, *65* (1-2), 55-63.
- 17 (35) Leroux, C.-E.; Grichine, A.; Wang, I.; Delon, A. Correction of cell induced optical
18 aberrations in a fluorescence fluctuation microscope. *Optics Letter* **2013**, *38* (14), 2401-2403.
- 19 (36) D'Este, M.; Eglin, D.; Alini, M. A Systematic Analysis of DMTMM vs EDC/NHS for
20 Ligation of Amines to Hyaluronan in Water. *Carbohydr. Polym.* **2014**, *108*, 239–246.
- 21 (37) Cayot, P.; Tainturier, G. The Quantification of Protein Amino Groups by the
22 Trinitrobenzenesulfonic Acid Method: A Reexamination. *Anal. Biochem.* **1997**, *249* (2), 184–
23 200.
- 24 (38) Ellis, G. A.; Palte, M. J.; Raines, R. T. Boronate-Mediated Biologic Delivery. *J. Am.*
25 *Chem. Soc.* **2012**, *134* (8), 3631–3634.
- 26 (39) Mouser, V. H. M.; Melchels, F. P. W.; Visser, J.; Dhert, W. J. A.; Gawlitta, D.; Malda, J.
27 Yield Stress Determines Bioprintability of Hydrogels Based on Gelatin-Methacryloyl and Gellan
28 Gum for Cartilage Bioprinting. *Biofabrication* **2016**, *8* (3), 035003.
- 29 (40) Chen, M. H.; Wang, L. L.; Chung, J. J.; Kim, Y.-H.; Atluri, P.; Burdick, J. A. Methods
30 To Assess Shear-Thinning Hydrogels for Application As Injectable Biomaterials. *ACS Biomater.*
31 *Sci. Eng.* **2017**, *3* (12), 3146–3160.

32

33

34

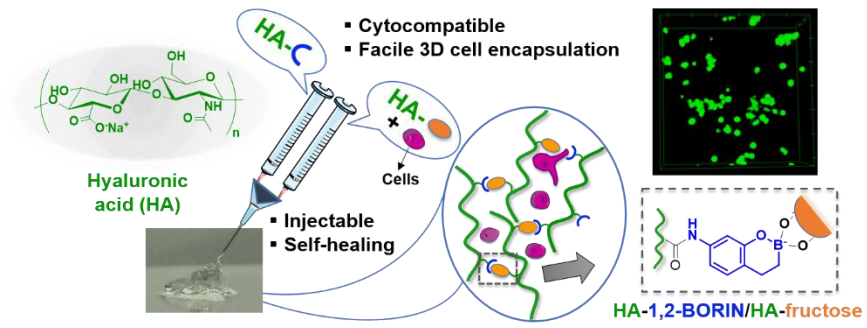
1

2

3

Table of Contents graphic

4



5